Int. J. Electrochem. Sci., 17 **(2022)** Article Number: 221162, doi: 10.20964/2022.11.62

International Journal of
ELECTROCHEMICAL
SCIENCE
www.electrochemsci.org

Short Communication

Effect of pH on corrosion behavior of Al-Mg-Si alloy in NaCl solution

Fen Xiao, Haichou Zhang[*]*, Lingnan Kong, Yaya Zheng, Xu Hu*

Department of Materials Engineering, Hunan University of Humanities, Science and Technology, Loudi 417000
[*]E-mail: 616786629@qq.com

Received: 3 July 2022 / *Accepted:* 6 September 2022 / *Published:* 20 October 2022

The effects of pH on the electrochemical properties and corrosion behavior of the Al-Mg-Si alloys were investigated by scanning electron microscopy (SEM), Potentiodynamic polarization and electrochemical impedance spectroscopy (EIS). The results show that the corrosion behavior of Al-Mg-Si alloys strongly depends on the pH of the solution. The Al-Mg-Si alloys is susceptible to two forms of corrosion, including pitting corrosion in acidic solutions, and general corrosion in alkalinity solutions. When Ph is 4, the E_{corr} and i_{corr} are -1352 mV and 9.78×10^{-4} μA cm^{-2} respectively; when pH is 10, the E_{corr} shifts negatively to -1413 mV, and the i_{corr} is 1.35×10^{-4} μA cm^{-2}. The corrosion resistance of the Al-Mg-Si alloys is the lowest, and the corrosion is the most serious in acidic solution. The lowest sensitivity of the Al-Mg-Si alloys in neutral solution results from the especially stable protective oxide layer.

Keywords: Al-Mg-Si alloy; corrosion behavior; pH; electrochemical performance

1. INTRODUCTION

Al-Mg-Si alloys are widely used in aerospace, automotive, navigation, and industrial areas due to their high strength-to-weight ratios and corrosion resistance. [1-3]. The microstructures of Al-Mg-Si alloys can be altered by heat treatment, including the precipitation of intermetallic compounds and precipitates. These precipitates would adversely influence the corrosion performance of the alloy by forming local anode/cathode areas (galvanic effects), hence promoting the occurrence of corrosion fatigue and/or cracking, which is regarded as one of the gravest catastrophes [4,5]. So that more and more researchers have focused on the study of corrosion behavior and mechanism of aluminium alloy to find better protective methods and technologies [6-8].

In fact, the passivation layer (natural or artificial) generated on the surface of aluminum and its alloys is an efficient barrier against metal dissolution and is typically resistant to corrosion in aqueous

solutions [9]. Because of the uneven chemical composition and microstructure of the alloy surface micro-area, corrosion frequently begins here, and local corrosion, such as pitting corrosion and intergranular corrosion, occurs [10]. In Al-Mg-Si alloys, two basic types of intermetallic compounds are the Mg_2Si phase and the FeMn-rich phase. Because these intermetallic compounds have different electrochemical characteristics than the aluminum matrix, preferential dissolution of the matrix or the intermetallic particles themselves occurs, resulting in localized pitting corrosion or intergranular corrosion in the alloy [11,12]. Birbilis et al.[13] discovered that Mg_2Si has a lower corrosion potential in neutral NaCl solution than the aluminum matrix, which acts electrochemically anodic. Mg_2Si dissolves itself by preferentially releasing Mg. It has also been discovered that Si enrichment may reverse the galvanic interaction between Mg_2Si and the Al matrix while simultaneously dissolving Mg. Luo et al.[14] demonstrated that the presence of the Mg_2Si phase may cause local pitting corrosion and even promote intergranular corrosion.

Recently, several researchers discovered that the corrosion environment can influence the corrosion development process of the Mg_2Si phase [15-17]. Kairy et al.[18] used electrochemical experiments to investigate the corrosion behavior of Al-Mg-Si alloys. The results revealed that corrosion occurred preferentially around the MgSi phase in NaCl solution with pH=3.5, and the main corrosion type is pitting corrosion. There have also been studies that demonstrate pitting corrosion of aluminum alloys is common phenomenon in the pH range of 2 to 10 [19-21]. Furthermore, alkaline corrosion is a required process prior to anodization. Investigating the corrosion of non-neutral areas has crucial practical implications for future heat treatment and further enhancing alloy corrosion resistance. Nabhan et al.[22] hypothesized that raising pH can accelerate corrosion kinetics strongly. Due to the non-uniform microstructure of AA6061, however, anodizing is frequently necessary to overcome the local corrosion problem. It is known little about the corrosion process of the alloy and the effect mechanism of corrosion rate induced by the solution pH, Some data on the influence of pH on the corrosion behavior of Al-Mg-Si alloys is still unclear.

Consequently, this work presents a study on corrosion behavior of the Al-Mg-Si alloys in 3.5 wt.% NaCl solution with different pH supported by evaluation of the electrochemical characteristic and microstructures. For this purpose, electrochemical, Scanning Electron Microscope (SEM) and transmission electron microscopy (TEM) analyses together to investigate the corrosion behavior of Al-Mg-Si alloys, as well as its polarization curve and AC impedance techniques aiming to establish a comprehensive EIS equivalent model to understand the corrosion mechanisms and corrosion kinetics. In addition, paying a particular attention to the dissolution of the second phases in different pH solution.

2. MATERIALS AND METHODS

The experimental alloys used in this research were made of high-purity Al, industrial pure Mg, high-purity Ag (99.99%), Al-50Sn, Al-16Mn, Al-20Si, Al-50Cu (wt.%), and other intermediate alloys that were smelted in a good resistance furnace. The chenmical compositions of the examined alloys are provided in Table 1. An ingot with a size of 45×25×30 mm was used. The ingot was homogenized at

520°C for 24 h, and each surface was cut to 5 mm thick. The alloy plate was subsequently solution treated at 550°C for 2 h. After that, the alloy plate was then immediately water-quenched to room temperature and artificially aged at 170°C for 4h. The sample dimensions are 3mm × 30mm × 10mm. Before the corrosion test, all samples were ground with 1200 and 2400 grit silicon carbide sandpaper, polished with 9mm, 3mm, and 1mm diamond paste, washed with ethanol, and dried. Three samples were corroded together in the same solution for each corrosion test. The average of three test samples' measurements. In this work, a 3.5 wt.% NaCl solution was utilized, and the pH of the solution was changed with NaOH and 1 mol/L HCl.

Table 1. The detailed chemical compositions of the studied Al-Mg-Si alloys

Mg	Si	Mn	Zr	Sn	Ti	Al
1.35	1.38	0.24	0.15	0.04	0.15	Bal.

Electrochemical experiments were performed at room temperature (25 °C) using a typical three-electrode electrochemical workstation. The alloy under investigation serves as the working electrode, the auxiliary electrode is a platinum sheet electrode, and the reference electrode is a saturated calomel electrode. All samples were cut into 10 mm 10 mm 8 mm cubes, and the pH of the electrolyte was changed using HCl and NaOH. The scanning speed is 2 mV/s. the scanning interval is -1500 mV~200 mV. Furthermore, electrochemical impedance spectroscopy (EIS) measurements were carried out in 3.5 wt.% NaCl solutions at various pH levels. the frequency range is 10 khz～0.1 hz. At steady state, electrochemical impedance spectroscopy (EIS) experiments were carried out. ZSimp Win software was used to fit EIS data with equivalent circuits (EECs). SEM was used to examine the alloys before and after corrosion.

3. RESULTS AND DISCUSSION

3.1 Open circuit potential

Open circuit potential (OCP) refers to the potential of the working electrode relative to the reference electrode when no current or potential in the cell [23,24]. Fig.1 shows the OCP versus time curves by immersing the samples in different pH NaCl solutions. The OCP of the samples moves in a negative way as the pH value increases or falls. In acidic solutions, the studied Al-Mg-Si alloy has a relatively stable OCP at around 1200 mV. In a pH=10 NaCl solution, the OCPs stable at roughly 1230 mV. The maximum OCP value is seen in a neutral solution with pH = 7.

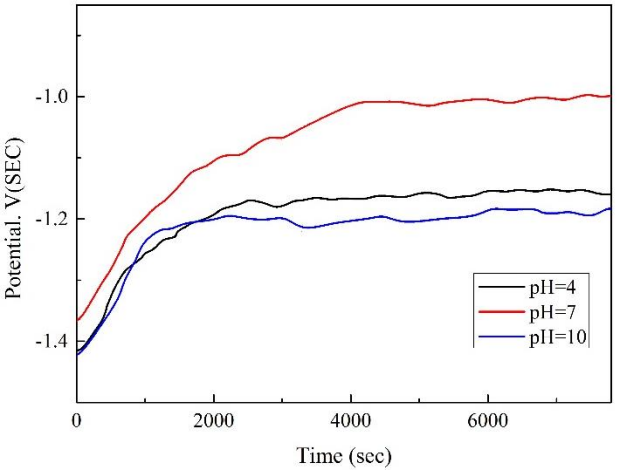

Figure 1. Effect of pH value on the OCP response.

3.2 Potentiodynamic polarisation test

Fig.2 depicts the polarization curves of Al-Mg-Si alloys in NaCl solutions with varying pH. The Tafel extrapolation technique of the cathode branch of the polarization curve was used to determine corrosion current density and other associated parameters at the self-corrosion potential. The results are shown in Table 2. The corrosion potential (E_{corr}) was -1142 mV when the solution pH was 7, and the corrosion current density (i_{corr}) was 1.91×10^{-5} μA cm^{-2}. As the pH value rises or falls, the passivation plateau of the anode branch shortens and the self-corrosion potential tends to decrease. When the pH of the solution was 10, the E_{corr} moved negatively by -1413 mV, and the i_{corr} was 1.35×10^{-4} μA cm^{-2}. When the pH of the solution reached 4, the E_{corr} moved negatively to -1.35 V, and the i_{corr} was 9.78×10^{-4} μA cm^{-2}.

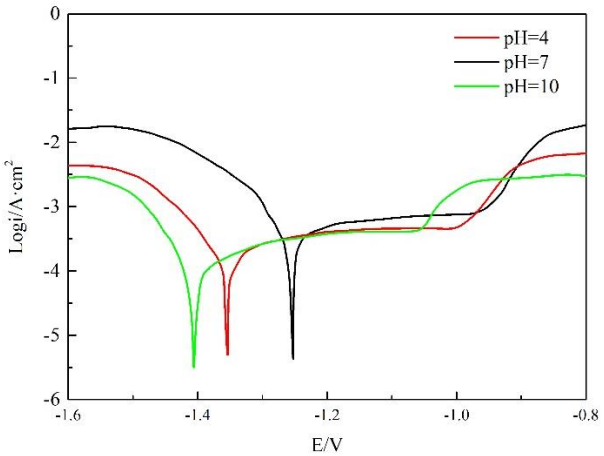

Figure 2. Polarization curves of the tested Al-Mg-Si alloys in different pH NaCl solution conducted at the steady state.

Table 2. Electrichemical data determined from polarization curves of the tested Al-Mg-Si alloys immersed in NaCl solution with different pH value

pH	E_{corr} (mV vs SCE)	E_{pit}(mV vs SCE)	$E_{pit} - E_{corr}$ (mV)	i_{corr} (μA cm^{-2})	β_a(mV/dec)	β_c(mV/dec)
4	-1352	-989±11	361	9.78×10^{-4}	85	121
7	-1142	-912±10	228	1.91×10^{-5}	82	129
10	-1413	-1093±13	317	1.35×10^{-4}	88	118

The corrosion parameters of the Al-Mg-Si alloys are shown in Table 2. The corrosion parameter revealed the following order of corrosion sensitivity of the Al-Mg-Si alloys: pH 7 < pH 4 < pH 10. Aluminum alloys have an amphoteric chemical reaction, which means they are soluble in acid and alkali solutions. The solubility of Al^{3+} in acidic solutions enhances the breakdown of the aluminum matrix. However, the corrosion process of aluminum alloys in neutral and alkaline media is connected to the creation of an aluminum hydroxide protective layer, and the high concentration of OH^- in alkaline solution dissolves and thins the oxide film evenly. In neutral solution, the passivation coating generated on the surface of the alloy by aluminum hydroxide ($Al(OH)_3$) is particularly stable due to its poor solubility.

3.3 Corrosion morphology

Fig.3 depicts the surface morphology of the alloy following the detection of the alloy's polarization curve. Fig.3a shows the alloy with several corrosion pits. When the pH was 7, the alloy displayed fewer corrosion spots and the majority of dense pits closely packed along grain boundaries are linked, but the grain surface is relatively intact. When the pH of the alloy reaches 10, When the pH is 10, the alloy exhibits general corrosion accompanied by a large number of corrosion pits.

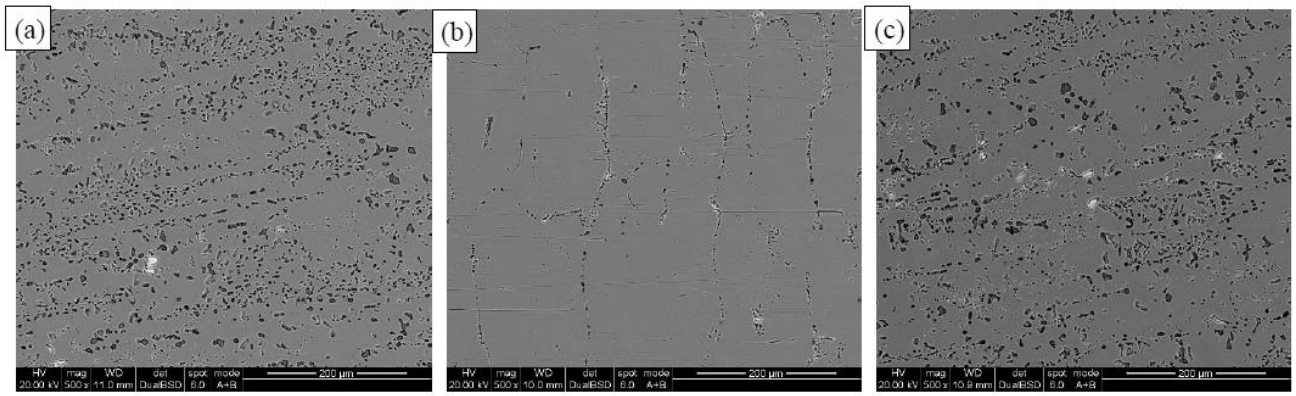

Figure 3. Corrosion morphology of the Al-Mg-Si alloy immersed in NaCl solution with different pH. (a) pH=4; (b) pH=7; (a) pH=10

3.4 Electrochemical impedance spectroscopy

Fig.5 depicts the electrochemical impedance spectroscopy (EIS) plots of Al-Mg-Si alloys in NaCl solutions with varying pH values. The high-frequency impedance spectra of an Al-Mg-Si alloy in NaCl solutions with varying pH levels revealed capacitive reactance arcs. The capacitive arc in lower frequency range can illustrate the breakdown of the oxide-film and porous deposit, such as $Al(OH)^{3+}$ ads, $Al(OH)^{2+}$ or $Al(OH)_3$, and can be viewed as an symbol of pitting corrosion. As the pH of the solution increased, the low-frequency sections gradually changed from capacitive reactance arcs to inductive reactance arcs. Table 3 displays the corresponding fitting parameters. The charge transfer resistance R1 of the alloy increases fast when the pH value decreases or increases, and i_{corr} increases significantly. When combined with the previous study' results that the oxidation product varies with pH, it is plausible to suppose that when the pH value rises, a considerable amount of hydroxide develops, resulting in broad-area dissolving corrosion of the aluminum matrix and an increase in the anodic reaction [13].

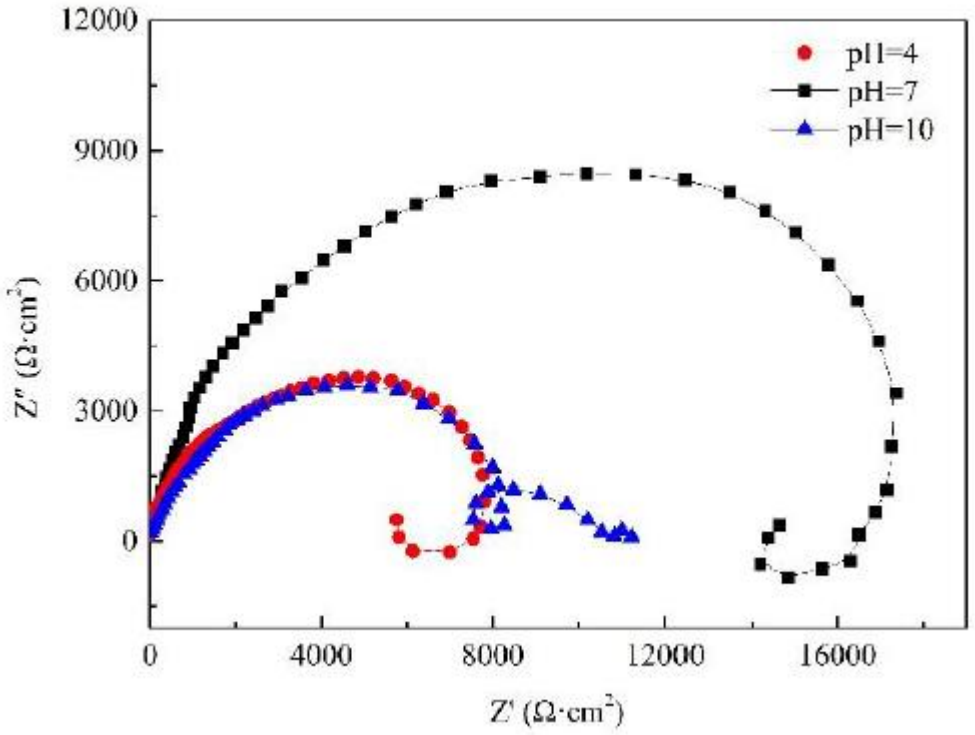

Figure 4. EIS curves of the Al-Mg-Si alloy immersed in NaCl solution with different pH at 25℃.

Fig. 5 shows two equivalent circuits used to illustrate the sample's corrosion behaviour. R_s, R_{sf}, and R_{ct} represent the solution, surface film, and charge transfer resistances, respectively; Q_1 and Q_2 represent the surface film and electric double layer capacitance constant phase angle elements, respectively; and L represents the relaxation process inductance element. The phenomenon is frequently linked with high Cl^- adsorption in limited corrosion zones, such as those surrounding the

second phase. Table 3 displays the corresponding electrochemical parameters obtained by extrapolating the Tafel slopes.

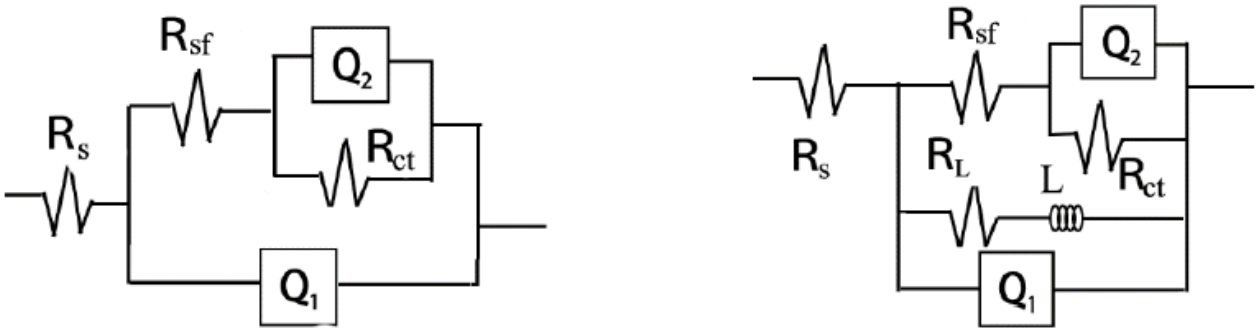

(a) (b)

Figure 5. Equivalent circuit of the EIS results. (a) pH=4 and pH=7; (b) pH =10

Table 3. EIS fitting parameters of the Al-Mg-Si alloy immersed in NaCl solution with different pH.

pH	$Q_1 \times 10^{-5}$ ($\Omega^{-1}s^n cm^{-2}$)	n	R_{surf} ($\Omega \cdot cm^{-2}$)	R_{ct} ($\Omega \cdot cm^{-2}$)
4	3.25	0.92	8431	4986
7	3.84	0.94	15677	7298
10	3.54	0.93	10562	6371

MnFe and MgSi intermetallic phases were observed on the surface. Surface flaws will inevitably emerge due to the presence of these intermetallics [25,26]. In neutral solution, intermetallic complexes such as MnFe operate as cathodes, causing corrosion of the surrounding Al matrix, PFZ, or MgSi anodic phase [27]. The release of Mg ions from Mg_2Si particle corrosion leads in the formation of SiO_2 in solution. The main anodic reactions are as follow:[28]

$$Mg \rightarrow Mg^{2+} + 2e^- \quad [1]$$

and the cathodic reactions occurred on pure Al are mainly hydrogen evolution reaction and oxygen reduction reaction, respectively [29,30].

$$2H+ + 2e^- \rightarrow H_2 \uparrow \quad [2]$$

$$O_2 + 2H_2O + 4e^- \rightarrow 4OH^- \quad [3]$$

Most of the Mg_2Si phase is completely separated from the Al matrix. In the corrosion process, Al will significantly promote Mg_2Si preferentially dealloying, and as the corrosion period grows, these enhancing effects decreases [31].

Electrochemical measurements revealed that the Mg_2Si phase dissolves quickly in acidic environments. These findings are consistent with those reported by Birbilis et al.[32] When the pH increases, the majority of the aluminum element exists in the solution as a positive ion. Depending on the pH of the solution, aluminum ion can quickly react with hydroxyl ion to generate insoluble hydroxide sediment or soluble hydroxyl complex (4)-(7) [32].

$$Al^{3+} + OH^- \rightarrow Al(OH)^{2+} \quad [4]$$

$$Al^{3+} + 2OH^- \rightarrow Al(OH)_2^+ \quad [5]$$

$$Al^{3+} + 3OH^- \rightarrow Al(OH)_3 \quad [6]$$

$$Al^{3+} + OH^- + 2Cl^- \rightarrow Al(OH)Cl_2^- \quad [7]$$

In addition, Alkaline solution has the ability to passivate magnesium. The main reactions as following:[33]

$$Mg + 2OH^- \rightarrow Mg(OH)_2 + 2e^- \quad [8]$$

$$Mg(OH)_2 \rightarrow MgO + H_2O \quad [9]$$

In alkaline solution, the Al-Mg-Si alloy corrodes with a slower rate than it does in acidic solution because the corrosion products deposit themselves on the surface of the corrosion [34]. Notably, when these corrosion products deposit in the opening of the corrosion pit, an occluded corrosion cell is formed, resulting in a lower pH value at the corrosion site's front. Corrosion continued along grain boundaries into the alloy's interior.

4. CONCLUSIONS

This paper puts an emphasis on the electrochemical performances and corrosion behavior of the Al-Mg-Si alloys in NaCl solution with different pH. The main conclusions can be drawn as follows:

1. The electrochemical performances and corrosion behavior of Al-Mg-Si alloys are greatly influenced by the pH of the NaCl solution. In Cl^- containing solutions with varying pH, distinct corrosion with different degrees occurred around the MnFe and MgSi phases.

2. When the pH of the NaCl solution is 4, the E_{corr} and of i_{corr} are -1.35 V and 9.78×10^{-4} μA cm^{-2}, respectively; when the pH of the NaCl solution is 10, the E_{corr} moves negatively to -1.41 V, and the i_{corr} is 1.35×10^{-4} μA cm^{-2}. The pH of the corrosive solution has a significant influence on the corrosion behavior of Al-Mg-Si alloys.

3. Under acidic or alkaline conditions, the Al-Mg-Si alloy displays large-area corrosion. When the pH of the NaCl solution is 7, the Al-Mg-Si alloy shows slight pitting corrosion and the lowest corrosion sensitivity.

ACKNOWLEDGEMENT
This work was sponsored in part by the scientific research project of education department of Hunan province (No.18A411; 18B452).

References

1. J. Xie, Y. Chen, L. Yin, T. Zhang, S. Wang and L. Wang, *J Manuf. Process*, 64 (2021) 473.
2. Y. Li, D.D. Macdonald, J. Yang, J. Qiu and S. Wang, *Corros. Sci*., 163 (2020) 108280.
3. H. Guan, S. Huang, J. Ding, F. Tian, Q. Xu and J. Zhao, *Acta Mater*., 187 (2020) 122.
4. M. Paz Martínez-Viademonte, S.T. Abrahami, T. Hack, M. Burchardt and H. Terryn, *Coatings*, 10 (2020) 1106.
5. S. Guo, J.J. Leavitt, X. Zhou, E. Lahti and J. Zhang, *RSC Advances*, 6 (2016) 44119.

6. V. Fallah, B. Langelier, N. Ofori-Opoku, B. Raeisinia, N. Provatas and S. Esmaeili, *Acta Mater*., 103(2016) 290.
7. Y.Y. Zheng, B.H. Luo, Z.H. Bai and C. He. *JOM*, 71(12) (2019) 4737.
8. B. Wang, X.H. Chen, F.S. Pan, J.J. Mao and Y. Fang, *Trans. Nonferrous Met. Soc. China*, 25 (8) (2015) 2481.
9. G.A. Zhang, L.Y. Xu and Y.F. Cheng, *Corros. Sci*., 51 (2) (2009) 283.
10. K. Khanari and M. Finšgar, *Arabian J. Chem*., 12 (8) (2019) 4646.
11. X. Joseph Raj and N. Rajendran, *J. Fail. Anal. Prev*., 19 (2019) 250.
12. M.G.A. Khedr and A.M.S. Lashien, *J. Electrochem. Soc*., 136 (4) (1989) 968.
13. W.J. Liang, P.A. Rometsch, L.F. Cao, N. Birbilis. *Corros. Sci*.,76 (2013) 119.
14. Y.Y. Zheng, B.H. Luo, C. He, Z.W. Ren, S. Wang and Y. Yuan. B. *Mater. Sci*., 42 (2019) 228.
15. M.Askari, M. Aliofkhazraei, S. Ghaffari and A. Hajizadeh, *J. Nat. Gas Sci. Eng*., 58 (2018) 92.
16. J. Xia, Z. Li, J. Jiang, X. Wang and X. Zhang, *Int. J. Electrochem. Sci*., 16 (2021) 210532.
17. N.R. Ramesh and V.S. Senthil Kumar, *Appl. Ocean Res*., 98 (2020) 102121.
18. K.S. Kairy, N. Birbilis, *Corros*., 76 (5) (2020) 464.
19. E. Irissou, J.G. Legoux, B. Arsenault and C. Moreau, *J. Therm. Spray Technol*., 16 (5) (2007) 661.
20. P. Huang, A. Somers, P.C. Howlett and M. Forsyth, *Surf. Coat. Technol*., 303 (2016) 385.
21. W. Liu, Q. Li and M.C. Li, *Corros. Sci*., 121 (2017) 72.
22. D. Nabhan, B. Kapusta, P. Billaud, K. Colas, D. Hamon and N. Dacheux, *J. Nucl. Mater*. 457 (2015) 196.
23. D. Persson, D. Thierry and N. Lebozec, *Corros. Sci.,* 53 (2) (2011) 720.
24. J. Mehta, V.K. Mittal and P. Gupta, *J. Appl. Sci. Process Eng*., 20 (4) (2017) 445.
25. I. Bakos and S. Szabó, *Corros. Sci*., 50 (1) (2008) 200.
26. J. Huang, Y. Liu, J.H. Yuan and H. Li, *J. Therm. Spray Technol*., 23 (4) (2014) 676.
27. Y.L. Lu, J. Wang, X.C. Li, W. Li, R. Li, D.S. Zhou, *Mater. Sci. Eng. A*, 723 (2018) 204.
28. M.S. Uddin, C.L. Hall, P. Murphy, *Sci. Technol. Adv. Mat*., 16 (2015) 053501
29. L.C. Córdoba, M.F. Montemor, T. Coradin, *Corros. Sci*., 104 (2016) 152.
30. R.F. Zhang, Y. Qiu, Y.S. Qi, N. Birbilis, *Corros. Sci*., 133 (2018) 1.
31. Y. Zou, Q. Liu, Zh. Jia, Y. Yuan, L.P. Ding, X.l. Wang, *Appl. Surf. Sci*., 405 (2017) 489.
32. P. Li, Y. Zhao, Y.Z. Liu, Y. Zhao, D. Xu, C.G. Yang, T. Zhang, T.Y. Gu, K. Yang, *J. Mater. Sci. Technol*., 33 (2017) 723.
33. F. Eckermann, T. Suter, P.J. Uggowitzer, A. Afseth, P. Schmutz, *Electrochim. Acta*, 54 (2008) 844.
34. B. Zaid, N. Maddache, D. Saidi, N. Souami, N. Bacha, A.Si Ahmed, *J. Alloys Compd*., 629 (2015) 188.